

# **Extracts of the 2011 Annual Report of the (former) JGU “Institute of Nuclear Chemistry”**

## **Upgrade of the gas-filled recoil separator TASCA and first search experiment for the new element 120 in the reaction $^{50}\text{Ti} + ^{249}\text{Cf}$**

**Page 2**

Ch.E. Düllmann, A. Yakushev, J. Khuyagbaatar, D. Rudolph, H. Nitsche, D. Ackermann, L.-L. Andersson, M. Block, D.M. Cox, J. Dvorak, K. Eberhardt, P.A. Ellison, N.E. Esker, J. Even, C. Fahlander, U. Forsberg, J.M. Gates, K.E. Gregorich, P. Golubev, O. Gothe, W. Hartmann, R.-D. Herzberg, F.P. Heßberger, J. Hoffmann, R. Hollinger, A. Hübner, E. Jäger, J. Jeppsson, B. Kindler, S. Klein, I. Kojouharov, J.V. Kratz, J. Krier, N. Kurz, S. Lahiri, B. Lommel, M. Maiti, R.R. Mändl, S. Minami, A. Mistry, C. Mokry, J.P. Omtvedt, G.K. Pang, I. Pysmenetska, D. Renisch, J. Runke, L.G. Sarmiento, M. Schädel, B. Schausten, A. Semchenkov, J. Steiner, P. Thörle-Pospiech, N. Trautmann, A. Türler, J. Uusitalo, D. Ward, N. Wiehl, M. Wegrzecki, V. Yakusheva

## **Background reduction in TASCA**

**Page 3**

J.M. Gates, K.E. Gregorich, L.-L. Andersson, Ch.E. Düllmann, J. Dvorak, J. Even, K. Eberhardt, U. Forsberg, D. Hild, E. Jäger, J. Jeppsson, J. Khuyagbaatar, J.V. Kratz, J. Krier, J.P. Omtvedt, I. Pysmenetska, D. Renisch, D. Rudolph, M. Schädel, A. Semchenkov, A. Vascon, N. Wiehl, A. Yakushev

## **Preparation of $^{249}\text{Cf}$ targets from pre-used material**

**Page 4**

J. Runke, Ch.E. Düllmann, K. Eberhardt, P.A. Ellison, K.E. Gregorich, E. Jäger, B. Kindler, J. Krier, B. Lommel, C. Mokry, H. Nitsche, M. Schädel, P. Thörle-Pospiech, N. Trautmann, Y. Yakushev

## **Targets for “TRAKULA”**

**Page 5**

A. Vascon, H. Christ, N. Wiehl, Ch.E. Düllmann, K. Eberhardt, J. Runke

## **Search for short-lived uranium isotopes around N=126**

**Page 6**

J. Khuyagbaatar, Ch.M. Mrosek, A. Yakushev, D. Ackermann, L.-L. Andersson, M. Block, D.M. Cox, Ch.E. Düllmann, J. Dvorak, K. Eberhardt, P.A. Ellison, N.E. Esker, J. Even, C. Fahlander, U. Forsberg, J.M. Gates, K.E. Gregorich, P. Golubev, O. Gothe, W. Hartmann, R.-D. Herzberg, F.P. Heßberger, J. Hoffmann, R. Hollinger, A. Hübner, E. Jäger, J. Jeppsson, B. Kindler, S. Klein, I. Kojouharov, J.V. Kratz, J. Krier, N. Kurz, S. Lahiri, B. Lommel, M. Maiti, R.R. Mändl, S. Minami, A. Mistry, C. Mokry, H. Nitsche, J.P. Omtvedt, G.K. Pang, I. Pysmenetska, D. Renisch, D. Rudolph, J. Runke, L.G. Sarmiento, M. Schädel, B. Schausten, A. Semchenkov, J. Steiner, P. Thörle-Pospiech, N. Trautmann, A. Türler, J. Uusitalo, D. Ward, N. Wiehl, M. Wegrzecki, V. Yakusheva

## **Preparations towards X-ray fingerprinting of element 115 decay chains**

**Page 7**

U. Forsberg, P. Golubev, L.G. Sarmiento, J. Jeppsson, D. Rudolph, L.L. Anderson, D. Ackermann, M. Asai, M. Block, K. Eberhardt, J. Even, Ch.E. Düllmann, J. Dvorak, J.M. Gates, K.E. Gregorich, R.D. Herzberg, F.P. Heßberger, E. Jäger, J. Khuyagbaatar, I. Kojouharov, J.V. Kratz, J. Krier, N. Kurz, S. Lahiri, B. Lommel, M. Maiti, E. Merchán, J. P. Omtvedt, E. Paar, J. Runke, H. Schaffner, M. Schädel, A. Yakushev

## **IRIS - feasibility calculations**

**Page 8**

J. Dvorak, Ch.E. Düllmann

## **Mass measurements of heavy actinides with SHIPTRAP**

**Page 9**

E. Minaya Ramirez, D. Ackermann, K. Blaum, M. Block, C. Droese, Ch.E. Düllmann, M. Dworschak, M. Eibach, S. Eliseev, E. Haettner, F. Herfurth, F.P. Heßberger, S. Hofmann, J. Ketelaer, J. Ketter, G. Marx, D. Nesterenko, Y. Novikov, W.R. Plass, D. Rodriguez, C. Scheidenberger, L. Schweikhard, P.G. Thirolf, G.K. Vorobjev, C. Weber

## **Metal carbonyl complexes – a new compound class accessible for transactinides**

**Page 10**

J. Even, A. Yakushev, Ch.E. Düllmann, J. Dvorak, R. Eichler, O. Gothe, D. Hild, E. Jäger, J. Khuyagbaatar, J.V. Kratz, J. Krier, L. Niewisch, H. Nitsche, I. Pysmenetska, M. Schädel, B. Schausten, A. Türler, N. Wiehl, D. Wittwer

## **Development of an on-line high-temperature surface ion source for fission products at TRIGA-SPEC**

D. Renisch, T. Beyer, K. Blaum, Ch.E. Düllmann, K. Eberhardt, M. Eibach, S. Klein, Sz. Nagy, W. Nörtershäuser, C. Smorra

**Page 11**

## **Resonance conditions of neutrinoless double-electron capture in cadmium and osmium isotopes investigated at TRIGA-TRAP**

**Page 12**

C. Smorra, T. Beyer, K. Blaum, M. Block, Ch. E. Düllmann, K. Eberhardt, M. Eibach, S. Eliseev, Sz. Nagy, W. Nörtershäuser and D. Renisch

# Upgrade of the gas-filled recoil separator TASCA and first search experiment for the new element 120 in the reaction $^{50}\text{Ti} + ^{249}\text{Cf}$

Ch.E. Düllmann<sup>1,2,3</sup>, A. Yakushev<sup>2</sup>, J. Khuyagbaatar<sup>2,3</sup>, D. Rudolph<sup>4</sup>, H. Nitsche<sup>5</sup>, D. Ackermann<sup>2</sup>, L.-L. Andersson<sup>3,6</sup>, M. Block<sup>2</sup>, D.M. Cox<sup>6</sup>, J. Dvorak<sup>3</sup>, K. Eberhardt<sup>1</sup>, P.A. Ellison<sup>5</sup>, N.E. Esker<sup>5</sup>, J. Even<sup>1,3</sup>, C. Fahlander<sup>4</sup>, U. Forsberg<sup>4</sup>, J.M. Gates<sup>5</sup>, K.E. Gregorich<sup>5</sup>, P. Golubev<sup>4</sup>, O. Gothe<sup>5</sup>, W. Hartmann<sup>2</sup>, R.-D. Herzberg<sup>6</sup>, F.P. Heßberger<sup>2,3</sup>, J. Hoffmann<sup>2</sup>, R. Hollinger<sup>2</sup>, A. Hübner<sup>2</sup>, E. Jäger<sup>2</sup>, J. Jeppsson<sup>4</sup>, B. Kindler<sup>2</sup>, S. Klein<sup>1</sup>, I. Kojouharov<sup>2</sup>, J.V. Kratz<sup>1</sup>, J. Krier<sup>2</sup>, N. Kurz<sup>2</sup>, S. Lahiri<sup>7</sup>, B. Lommel<sup>2</sup>, M. Maiti<sup>7</sup>, R.R. Mändl<sup>2,8</sup>, S. Minami<sup>2</sup>, A. Mistry<sup>6</sup>, C. Mokry<sup>1</sup>, J.P. Omtvedt<sup>9</sup>, G.K. Pang<sup>5</sup>, I. Pysmenetska<sup>2</sup>, D. Renisch<sup>1</sup>, J. Runke<sup>2</sup>, L.G. Sarmiento<sup>10</sup>, M. Schädel<sup>2,11</sup>, B. Schausten<sup>2</sup>, A. Semchenkov<sup>9</sup>, J. Steiner<sup>2</sup>, P. Thörle-Pospiech<sup>1</sup>, N. Trautmann<sup>1</sup>, A. Türler<sup>12</sup>, J. Uusitalo<sup>13</sup>, D. Ward<sup>4</sup>, N. Wiehl<sup>1</sup>, M. Wegrzecki<sup>14</sup>, V. Yakusheva<sup>3</sup>

<sup>1</sup>U. Mainz, Germany, <sup>2</sup>GSI, Darmstadt, Germany, <sup>3</sup>HIM, Mainz, Germany, <sup>4</sup>Lund U, Sweden, <sup>5</sup>LBNL+UC Berkeley, CA, USA, <sup>6</sup>U. Liverpool, UK, <sup>7</sup>SINP, Kolkata, India, <sup>8</sup>FH Frankfurt, <sup>9</sup>U. Oslo, Norway, <sup>10</sup>UNAL Bogotá, Colombia, <sup>11</sup>JAEA Tokai, Japan, <sup>12</sup>U. Bern+PSI Villigen, Switzerland <sup>13</sup>U. Jyväskylä, Finland, <sup>14</sup>ITE Warsaw, Poland

The heaviest elements were discovered in  $^{48}\text{Ca}$ -induced fusion reactions with actinide targets [1]. The observation of the hitherto heaviest element 118 was claimed from irradiations of targets of  $^{249}\text{Cf}$ , which is the highest-Z nucleus that is available in sufficient quantities. Hence, to search for elements beyond  $Z=118$ , reactions induced by projectiles with  $Z>20$  are required. Previously,  $^{64}\text{Ni}+^{238}\text{U}$  [2],  $^{58}\text{Fe}+^{244}\text{Pu}$  [3], and recently  $^{54}\text{Cr}+^{248}\text{Cm}$  [4] were studied, but element 120 is yet to be discovered. Theoretical predictions [5-8] agree on the  $^{50}\text{Ti}+^{249}\text{Cf}$  reaction to have the highest cross section. Accordingly, the TASCAs collaboration selected this reaction to search for element 120. Maximum predicted cross sections range from 0.04 pb [5] to 0.75 pb [6, 8]. For comparison, the  $^{48}\text{Ca}+^{249}\text{Cf} \rightarrow Z=118$  experimental cross section is  $0.5_{-0.3}^{+1.6}$  pb [9].

On the way to a first search experiment for element 120 at TASCAs, upgrades of several key components were performed, compared to the setup as used for the  $^{244}\text{Pu}(^{48}\text{Ca},3\text{-}4\text{n})^{288,289}\text{114}$  reaction [10, 11]. These include the implementation of a larger-area target wheel with 100 mm diameter comprising four targets [12]. The heat of each 5-ms long UNILAC macropulse is now dissipated over a four times larger area ( $6\text{ cm}^2$ ) than in the old system ( $1.4\text{ cm}^2$ ) used for element 114.

The separation from unwanted nuclear reaction products was increased by a factor of  $\sim 10$  [13] by (i) implementing a carbon stripper foil in front of the target to increase the beam charge state, (ii) a fixed scraper mounted in the center of the first quadrupole magnet, and (iii) a second, moveable scraper mounted behind the second quadrupole. Both scraper positions were chosen based on ion-optical simulations, which predicted significant background suppression without loss in EVR efficiency due to the scrapers. Measurements, e.g., of the  $^{48}\text{Ca}+^{208}\text{Pb}$  reaction, confirmed the expectations (see also [14]). The efficiency of TASCAs for element 120 produced in the reaction  $^{50}\text{Ti}+^{249}\text{Cf}$  was calculated to be  $(62\pm 6)\%$ . Discrimination between various event types was enhanced by improving the multi-wire proportional counter veto detector

efficiency compared to the element 114 experiment. Several predictions of decay properties of isotopes produced in the  $^{50}\text{Ti}+^{249}\text{Cf}$  reaction suggest their half-lives,  $T_{1/2}$ , to be on the order of  $\mu\text{s}$ . This is shorter than the dead-time of the data acquisition (DAQ) system used in 2009 [11]. Therefore, a fast digital sampling pulse processing system was built and integrated into the DAQ system [15]. This allowed registering events with  $T_{1/2}$  as short as 100 ns, as confirmed in a study of the reaction  $^{50}\text{Ti}+^{176}\text{Yb}$ , which yields decay chains with very short-lived members [16].

Old  $^{249}\text{Cf}$  samples were chemically reprocessed and electrodeposited on  $\sim 2.2\text{-}\mu\text{m}$  thick Ti backings by molecular plating [17], yielding  $\sim 0.5\text{-mg/cm}^2$  thick targets.

In August-October 2011, a first experiment to search for element 120 was conducted. Intense beams ( $0.5\text{-}1.0\text{ }\mu\text{A}_{\text{part}}$ ) were applied on the Cf targets during 39 days of beamtime. The data analysis is in progress.

*Acknowledgments:* We thank the ion source and accelerator staff for providing stable and intense  $^{50}\text{Ti}$  beams, and the experimental electronics department for making the digital DAQ system available on a short time-scale.

## References

- [1] Y. Oganessian, *Radiochim. Acta* **99**, 429 (2011).
- [2] S. Hofmann *et al.*, *GSI Sci. Rep.* 2008 (2009) p. 131.
- [3] Yu.Ts. Oganessian *et al.*, *Phys. Rev. C* **79**, 024603 (2009).
- [4] S. Hofmann *et al.*, this Scientific Report (2012).
- [5] V. Zagrebaev *et al.*, *Phys. Rev. C* **78**, 034610 (2008).
- [6] G. G. Adamian *et al.*, *Eur. Phys. J. A* **41**, 235 (2009).
- [7] A. K. Nasirov *et al.*, *Phys. Rev. C* **84**, 044612 (2011).
- [8] K. Siwek-Wilczynska *et al.*, *IJMPPE* **19**, 500 (2010).
- [9] Yu.Ts. Oganessian *et al.*, *Phys. Rev. C* **74**, 044602 (2006).
- [10] Ch.E. Düllmann *et al.*, *Phys. Rev. Lett.* **104**, 252701 (2010).
- [11] J.M. Gates *et al.*, *Phys. Rev. C* **83**, 054618 (2011).
- [12] T. Torres *et al.*, *GSI Sci. Rep.* 2010 (2011) p. 236.
- [13] J. M. Gates *et al.*, this Scientific Report (2012).
- [14] U. Forsberg *et al.*, this Scientific Report (2012).
- [15] N. Kurz *et al.*, this Scientific Report (2012).
- [16] J. Khuyagbaatar *et al.*, this Scientific Report (2012).
- [17] J. Runke *et al.*, this Scientific Report (2012).

## Background Reduction in TASCA

*J.M. Gates*<sup>1, #</sup>, *K.E. Gregorich*<sup>1</sup>, *L.-L. Andersson*<sup>2</sup>, *Ch.E. Düllmann*<sup>3,4,5</sup>, *J. Dvorak*<sup>5</sup>, *J. Even*<sup>3,5</sup>, *K. Eberhardt*<sup>3</sup>, *U. Forsberg*<sup>6</sup>, *D. Hild*<sup>3</sup>, *E. Jäger*<sup>4</sup>, *J. Jeppsson*<sup>6</sup>, *J. Khuyagbaatar*<sup>4,5</sup>, *J.V. Kratz*<sup>3</sup>, *J. Krier*<sup>4</sup>, *J.P. Omtvedt*<sup>7</sup>, *I. Pysmenetska*<sup>4</sup>, *D. Renisch*<sup>3</sup>, *D. Rudolph*<sup>6</sup>, *M. Schädel*<sup>4,8</sup>, *A. Semchenkov*<sup>7</sup>, *A. Vascon*<sup>3</sup>, *N. Wiehl*<sup>3</sup>, *A. Yakushev*<sup>4</sup>

<sup>1</sup>LBNL, Berkeley, CA, U.S.A., <sup>2</sup>U. Liverpool, UK, <sup>3</sup>U. Mainz, Germany, <sup>4</sup>GSI, Darmstadt, Germany, <sup>5</sup>HIM, Mainz, Germany, <sup>6</sup>Lund U., Sweden, <sup>7</sup>U. Oslo, Norway, <sup>8</sup>JAEA Tokai, Japan

During the  $^{244}\text{Pu}(^{48}\text{Ca}, 3-4n)^{289-288}$  114 experiment, high background rates in TASCA were observed and attributed to (i) transfer reaction products (TRPs) that have a magnetic rigidity (Bp) only  $\sim 15-30\%$  less than the evaporation residues (EVRs) of interest and decay properties similar to the EVRs and (ii) primary beam passing through pinholes in the target and entering TASCA without charge-exchange or scattering reactions [1]. Both TRPs and primary beam are separated from the evaporation residues (EVRs) of interest in the dipole, but a small fraction are guided back to the focal plane detector by the horizontally focusing quadrupole. This is shown in Fig. 1 for primary beam as compared to EVRs.

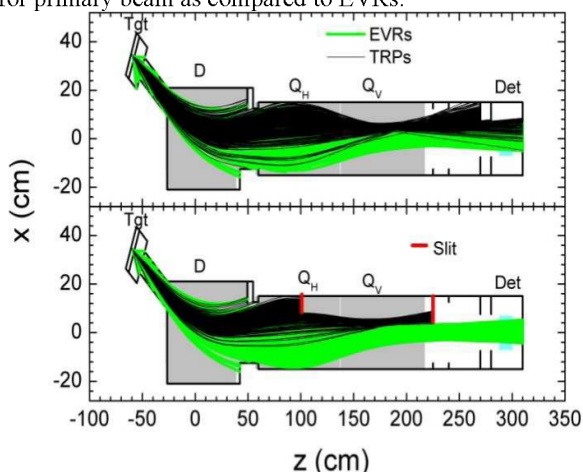


Fig. 1: Primary beam and EVR trajectories in TASCA.

Simulations [2] showed that separation between EVRs and background occurs at the center of the first quadrupole (Q1) and at the exit of TASCA. The use of strategic slits to reduce the acceptance of TASCA in these two areas was expected to result in significantly reduced background without large losses in EVR transmission efficiency as shown in the bottom of Fig. 1. Two solutions (hereafter referred to as M1 and M2) for reducing background in TASCA are:

M1. Introduction of a slit at the center of Q1 reaching from the low Bp side of TASCA to 8 cm from center. This was expected to result in reductions of 4, 90 and 98% for EVRs, TRPs and primary beam.

M2. M1 plus a slit at the exit of TASCA reaching from the low Bp side of TASCA to 3.5 cm from center. This was expected to result in reductions of 5, 97 and 99% for EVRs, TRPs and primary beam.

In April 2011, M1 and M2 were tested using the  $^{208}\text{Pb}(^{40}\text{Ar}, xn)$  reaction, chosen to represent ‘fast’ recoils where the Bp of the EVRs is approximately 15-30% higher than the Bp of the TRPs or primary beam. This is similar to what would be expected in reactions such as those currently being investigated to produce elements 119 and 120:  $^{249}\text{Bk}(^{50}\text{Ti}, xn)$  and  $^{249}\text{Cf}(^{50}\text{Ti}, xn)$  and the TASISpec element 115 X-ray Fingerprinting experiment.

The high and low energy spectra during the macropulse and the low energy spectra outside of the macropulse for unmodified TASCA, and TASCA with M1 and M2 are shown in Fig. 2. Background reductions of 77 and 84% for TRPs and primary beam, respectively, were observed with M1. For M2, reductions of 93 and 96% were observed for TRPs and primary beam, respectively, in fair agreement with the simulations. Rates of all events in the macropulse were reduced 65 and 88% for M1 and M2, respectively, while the outside of macropulse event rate for M1 and M2 was reduced by 75 and 89%, respectively. The experimental change in EVR transmission efficiency could not be quantified due to the low  $^{208}\text{Pb}(^{40}\text{Ar}, xn)$  cross section and interference from TRPs.

Without modification, the rate of events in the focal plane detector during the  $^{208}\text{Pb}(^{40}\text{Ar}, xn)$  reaction was 2900 Hz during the macropulse and 40 Hz outside of the macropulse. With the addition of either M1 or M2, these rates were reduced to  $<200$  Hz inside and  $<3$  Hz outside of the macropulse.

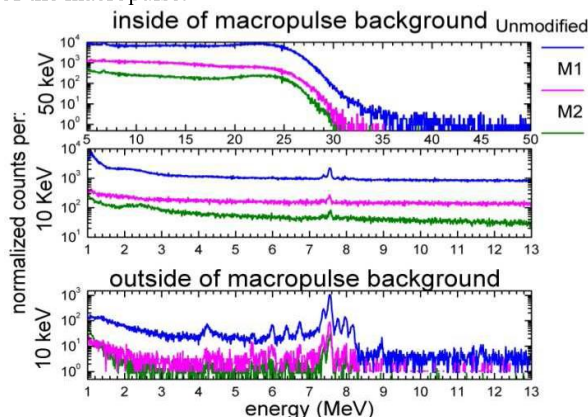


Fig. 2: Total energy spectra for TASCA unmodified and after M1-M2, normalized to the beam integral.

### References:

- [1] J.M. Gates *et al.*, Phys. Rev. C **83**, 054618 (2011)
- [2] K.E. Gregorich *et al.*, Phys. Rev. C **71**, 014605 (2005)

# Preparation of $^{249}\text{Cf}$ targets from pre-used material

J. Runke<sup>1</sup>, Ch.E. Düllmann<sup>1,2,3</sup>, K. Eberhardt<sup>2</sup>, P.A. Ellison<sup>4,5</sup>, K.E. Gregorich<sup>4</sup>, E. Jäger<sup>1</sup>,  
B. Kindler<sup>1</sup>, J. Krier<sup>1</sup>, B. Lommel<sup>1</sup>, C. Mokry<sup>2</sup>, H. Nitsche<sup>4,5</sup>, M. Schädel<sup>6</sup>, P. Thörle-Pospiech<sup>2</sup>,  
N. Trautmann<sup>2</sup>, A. Yakushev<sup>1</sup>

<sup>1</sup>GSI Helmholtzzentrum für Schwerionenforschung GmbH, Darmstadt, Germany; <sup>2</sup>Johannes Gutenberg-Universität Mainz, Germany; <sup>3</sup>Helmholtz-Institut Mainz, Germany; <sup>4</sup>Lawrence Berkeley National Laboratory, Berkeley, CA, USA; <sup>5</sup>University of California, Berkeley, CA, USA; <sup>6</sup>Advanced Science Research Center, Japan Atomic Energy Agency, Tokai, Japan

For the synthesis of the new element with atomic number  $Z = 120$ , the fusion reaction of  $^{50}\text{Ti}$  with  $^{249}\text{Cf}$  was studied at the gas-filled recoil separator TASCA [1]. Pre-used  $^{249}\text{Cf}$ , originating from the decay of  $^{249}\text{Bk}$ , was provided by the Lawrence Berkeley National Laboratory to produce suitable targets.

The chemical form of the delivered  $^{249}\text{Cf}$  was either the oxide, chloride or the nitrate. In a first step the material was dissolved in 8 M HCl. The  $^{249}\text{Cf}$  solution contained Al, Fe, Pb and Ti as impurities. In a first purification step the anion-exchanger BioRad AG MP-1M was applied to remove Al and Fe from the solution. In the second step a cation exchange column with DOWEX 50WX8 was used for the removal of Pb and Ti. Over both purification steps the Cf recovery was almost 100 %.

A rotating target wheel assembly was used, which was previously tested to accept high beam intensities up to 2  $\mu\text{A}$  (particle). Molecular plating (MP) [2] was employed for the preparation of  $^{249}\text{Cf}$  layers on  $\sim 2.2\text{-}\mu\text{m}$  thick Ti backing foils produced by cold rolling at GSI.

The average foil thickness was determined by weighing, whereas the homogeneity of the foil thickness was checked by  $\alpha$ -particle energy-loss measurements over 5 positions per foil. The standard deviation of the foil thickness varied between 0.03 and 0.14  $\mu\text{m}$ .

The deposition parameters for Cf were optimized in experiments with Gd. This also included MP with  $^{153}\text{Gd}$ -tracer to verify the homogeneity of the Gd layer using a commercial radiographic imager [3] (FLA 7000 from FUJIFILM Corp.).

The first step in the MP of Cf was the conversion of the Cf chloride into the nitrate by evaporation to dryness and re-dissolution in 8 M  $\text{HNO}_3$ . An aliquot of the Cf-solution with about 3 mg of  $^{249}\text{Cf}$  (455 MBq) was evaporated to dryness in a Teflon<sup>TM</sup> beaker. The green residue was re-dissolved in a small volume (100  $\mu\text{l}$ ) of 0.1 M  $\text{HNO}_3$ . The solution was transferred into an electrochemical deposition cell (EDC) made of PEEK. The beaker was washed with 3 x 300  $\mu\text{l}$  isopropanol, which was also transferred to the EDC. The EDC was filled up to a volume of 52 ml with isobutanol. For the mixing during the deposition process an ultrasonic stirrer was used [3]. For the MP of  $^{249}\text{Cf}$  with a surface of 6  $\text{cm}^2$  a voltage of 200 – 600 V at a maximum current density of about 0.3  $\text{mA}/\text{cm}^2$  was applied. The deposition time was 4 – 5 hours. The deposition yield exceeded 90 %. Fig. 1 shows one of the produced target segments.

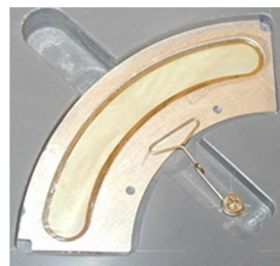


Figure 1: Cf target-segment

Prior to the production of  $\sim 0.5\text{-mg}/\text{cm}^2$  thick  $^{249}\text{Cf}$  targets, a thin  $^{249}\text{Cf}$  target was prepared. With this target we tested the deposition parameters. Before the deposition, and in 1-h steps during the MP process, 10  $\mu\text{l}$  aliquots of the  $^{249}\text{Cf}$ -solution were evaporated to dryness for  $\alpha$ -particle spectroscopy. With these measurements the decreasing Cf content in the solution during the deposition was determined as well as the deposition yield.

As a method for the yield determination,  $\gamma$  spectroscopy was used. For this, the thin  $^{249}\text{Cf}$  target served as a reference sample. The distance from the target to the  $\gamma$  detector was about 3 m, the dead time was 5%. The data confirmed a thickness of  $\sim 0.5\text{-mg}/\text{cm}^2$ , and the final analysis of the thickness values, including measurements performed after the element 120 experiment [1], is in progress.

*Acknowledgments:* We would like to thank Robert F. Fairchild II, Naomi E. Reeves, John A. van Wart and LBNL's entire Radiation Protection Group of the Environmental Health and Safety Division for their leadership and active support with the preparation and execution of the  $^{249}\text{Cf}$  shipment to Germany. This work was supported by the Helmholtz Institute Mainz.

## References

- [1] Ch.E. Düllmann et al., this scientific report (2012).
- [2] K. Eberhardt et al., Nucl. Instrum. Meth. Phys. Res. A590, 134 (2008).
- [3] A. Vascon et al., Nucl. Instrum. Meth. Phys. Res. A655, 72 (2011).

# Targets for “TRAKULA”\*

A. Vascon<sup>1</sup>, H. Christ<sup>2</sup>, N. Wiehl<sup>1</sup>, Ch.E. Düllmann<sup>1,3,4</sup>, K. Eberhardt<sup>1</sup>, J. Runke<sup>3</sup>

<sup>1</sup>Institute of Nuclear Chemistry, Johannes Gutenberg University Mainz, 55099 Mainz, Germany

<sup>2</sup>Institute of Physical Chemistry, Johannes Gutenberg University Mainz, 55099 Mainz, Germany

<sup>3</sup>SHE Chemistry Department, GSI Helmholtzzentrum für Schwerionenforschung GmbH, 64291 Darmstadt, Germany

<sup>4</sup>Helmholtz Institut Mainz, 55099 Mainz, Germany

Within the TRAKULA project (Transmutationsrelevante kernphysikalische Untersuchungen langlebiger Aktinide) which requires large-area samples ( $\geq 40 \text{ cm}^2$ ) of  $^{235,238}\text{U}$  and  $^{239,242}\text{Pu}$  to calibrate fission chambers and to measure neutron-induced fission yields for transmutation studies [1], large area targets of  $^{nat}\text{U}$  were prepared. Moreover, according to the need of targets for precise measurements of the half-life,  $t_{1/2}$ , of very long-lived  $\alpha$ -particle emitters like  $^{144}\text{Nd}$  ( $t_{1/2} \approx 2 \cdot 10^{15} \text{ y}$ ),  $^{nat}\text{Nd}$  samples with different surface properties were produced.

$^{nat}\text{U}$  targets were prepared using 250- $\mu\text{m}$  thick circular Ti backings with an area of  $43 \text{ cm}^2$ . The targets were prepared by Molecular Plating (MP) using  $^{nat}\text{UO}_2(\text{NO}_3)_3 \cdot 6\text{H}_2\text{O}$ . This salt was dissolved in 0.1M  $\text{HNO}_3$  and 200  $\mu\text{l}$  of this solution (5.7 mg of elemental U) were inserted inside the plating cell. This was then filled with 230 ml of isopropanol.  $^{nat}\text{Nd}$  targets were prepared on two circular Ti backings with different surface roughness to investigate the influence of a different surface structure on the quality of the deposited layers. One was a 50- $\mu\text{m}$  thick Ti foil with an average roughness of 20 nm, while the smoother one was a 300- $\mu\text{m}$  thick Ti coated Si wafer with an average roughness of 10 nm. The deposition area of these samples was  $9 \text{ cm}^2$  and for this reason a smaller volume cell was used. The MPs were realized using  $^{nat}\text{Nd}(\text{NO}_3)_3 \cdot 6\text{H}_2\text{O}$ . This salt was dissolved in 0.1M  $\text{HNO}_3$  and 100  $\mu\text{l}$  of this solution (containing 1.1 mg of elemental Nd) were inserted inside the plating cell. This was then filled with 1 ml of isopropanol and 34 ml of isobutanol. In both cases a constant current density of  $0.6 \text{ mA/cm}^2$  was applied for the production of the targets. The deposition time was 3 hours. The solution was mixed via ultrasonic stirring. The temperature was kept constant ( $14^\circ\text{C}$ ) using water-cooling.

The deposition yield was determined by Neutron Activation Analysis (NAA) and  $\gamma$ -spectroscopy. The 106 keV  $\gamma$ -line resulting from the 23-min decay of  $^{239}\text{U}$  into 2.4-d  $^{239}\text{Np}$  was used to determine the U content in 2 ml samples of the supernatant solution taken before and after the deposition process. The 2 ml extracted from the deposition cell before the plating process were used as standard reference. This sample volume represents less than 1% of the total volume of solution inside the cell and corresponds to a negligible loss of material for the deposition ( $\sim 50 \mu\text{g}$  of U from a total amount of 5.7 mg).

The evaluated deposition yield of the produced  $^{nat}\text{U}$  targets was very high:  $(99.921 \pm 0.021)\%$ . Gamma spectroscopy was used for the  $^{nat}\text{Nd}$  targets after active MPs, (i.e. depositions realized using a radioactive tracer  $^{147}\text{Nd}$ - inside the plating solution). The 91 keV  $\gamma$ -line of the  $\beta$ -decaying  $^{147}\text{Nd}$  was used as a reference during the  $\gamma$ -measurements of the standards and of the samples.

The standards were obtained by soaking a filter paper with the same geometry as the targets with the tracer-containing solution. The evaluated deposition yield was very high in both cases:  $(95.6 \pm 2.7)\%$  for the  $^{nat}\text{Nd}$  target produced on the Ti foil, and  $(98.7 \pm 0.8)\%$  for the  $^{nat}\text{Nd}$  target produced on the Ti coated Si wafer.

The homogeneity of the radioactive targets was inspected by using Radiographic Imaging (RI), using a FUJIFILM FLA 7000.

Taking into account the different deposition areas, the obtained yields, and the homogeneities as evaluated in the RI investigations, the areal density of the produced  $^{nat}\text{U}$  targets was  $(132 \pm 13) \mu\text{g/cm}^2$ . For the  $^{nat}\text{Nd}$  target produced on the Ti foil it was  $(117 \pm 12) \mu\text{g/cm}^2$ , and for the  $^{nat}\text{Nd}$  target produced on the Ti coated Si wafer it was  $(121 \pm 12) \mu\text{g/cm}^2$ .

The surface roughness of the  $^{nat}\text{Nd}$  targets was investigated by using an Atomic Force Microscope (AFM) (MFP 3D, Asylum Research) in tapping mode. Fig. 1 a and b show the AFM image of the Nd target produced on the Ti foil (mean roughness 120 nm) (a), and on the Ti coated Si wafer (mean roughness 65 nm) (b). From these results follows that smoother backings lead to smoother layers.

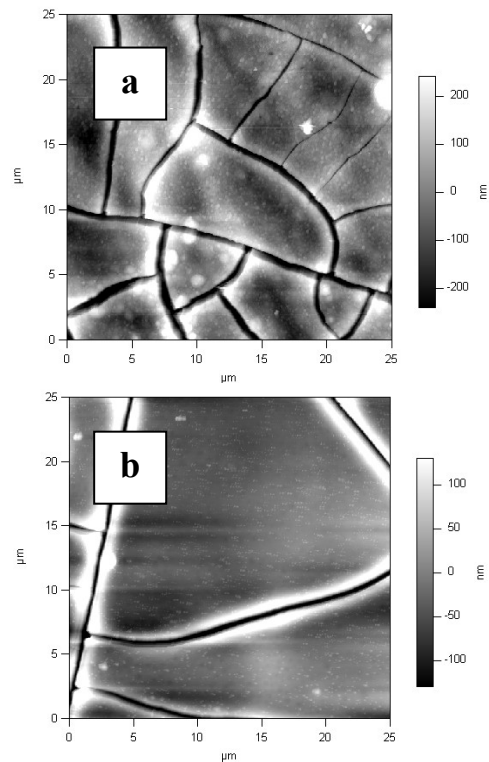


Figure 1: AFM picture of a  $^{nat}\text{Nd}$  target produced on a Ti foil (a) and on a Ti coated Si wafer (b).

## References

[1] A.Vascon et al., Nucl. Instrum. Meth. A **655** (2011) 72.

\* work supported by BMBF, contract number 02NUK013E.

## Search for short-lived uranium isotopes around N=126 \*

J. Khuyagbaatar<sup>1,2</sup>, Ch.M. Mrosek<sup>3</sup>, A. Yakushev<sup>1</sup>, D. Ackermann<sup>1</sup>, L.-L. Andersson<sup>2,4</sup>, M. Block<sup>1</sup>, D.M. Cox<sup>4</sup>, Ch.E. Düllmann<sup>1,2,3</sup>, J. Dvorak<sup>2</sup>, K. Eberhardt<sup>3</sup>, P.A. Ellison<sup>5</sup>, N.E. Esker<sup>5</sup>, J. Even<sup>2,3</sup>, C. Fahlander<sup>6</sup>, U. Forsberg<sup>6</sup>, J.M. Gates<sup>5</sup>, K.E. Gregorich<sup>5</sup>, P. Golubev<sup>6</sup>, O. Gothe<sup>5</sup>, W. Hartmann<sup>1</sup>, R.-D. Herzberg<sup>4</sup>, F.P. Heßberger<sup>1,2</sup>, J. Hoffmann<sup>1</sup>, R. Hollinger<sup>1</sup>, A. Hübner<sup>1</sup>, E. Jäger<sup>1</sup>, J. Jeppsson<sup>6</sup>, B. Kindler<sup>1</sup>, S. Klein<sup>3</sup>, I. Kojouharov<sup>1</sup>, J.V. Kratz<sup>3</sup>, J. Krier<sup>1</sup>, N. Kurz<sup>1</sup>, S. Lahiri<sup>7</sup>, B. Lommel<sup>1</sup>, M. Maiti<sup>7</sup>, R.R. Mändl<sup>1,8</sup>, S. Minami<sup>1</sup>, A. Mistry<sup>4</sup>, C. Mokry<sup>3</sup>, H. Nitsche<sup>5</sup>, J.P. Omtvedt<sup>9</sup>, G.K. Pang<sup>5</sup>, I. Pysmenetska<sup>1</sup>, D. Renisch<sup>3</sup>, D. Rudolph<sup>6</sup>, J. Runke<sup>1</sup>, L.G. Sarmiento<sup>10</sup>, M. Schädel<sup>1,11</sup>, B. Schausten<sup>1</sup>, A. Semchenkov<sup>9</sup>, J. Steiner<sup>1</sup>, P. Thörle-Pospiech<sup>3</sup>, N. Trautmann<sup>3</sup>, A. Türler<sup>11</sup>, J. Uusitalo<sup>13</sup>, D. Ward<sup>6</sup>, N. Wiehl<sup>3</sup>, M. Wegrzecki<sup>14</sup>, V. Yakusheva<sup>2</sup>

<sup>1</sup>GSI, Darmstadt, Germany, <sup>2</sup>HIM, Mainz, Germany, <sup>3</sup>U. Mainz, Germany, <sup>4</sup>U. Liverpool, UK, <sup>5</sup>LBNL+UC Berkeley, CA, USA, <sup>6</sup>Lund U. Sweden, <sup>7</sup>SINP, Kolkata, India, <sup>8</sup>FH Frankfurt, <sup>9</sup>U. Oslo, Norway, <sup>10</sup>UNAL Bogotá, Colombia, <sup>11</sup>JAEA Tokai, Japan, <sup>12</sup>U. Bern+PSI Villigen, Switzerland <sup>13</sup>U. Jyväskylä, Finland, <sup>14</sup>ITE Warsaw, Poland,

Production and decay of short-lived <sup>221</sup>U (previously unknown) and <sup>222</sup>U (only the half-life is known) were studied at the gas-filled separator TASCA. These two nuclei have only few neutrons more than the magic number N=126, which leads to high  $\alpha$  decay Q-values and, therefore, to very short half-lives (< 10  $\mu$ s). To explore this microsecond/sub-microsecond half-life region, digital electronics was implemented into a combined “ANalog” and “DigiTal” (ANDI) data acquisition system [1].

A <sup>50</sup>Ti<sup>12+</sup> beam was accelerated to energies  $E_{\text{lab}}=230$  and 240 MeV and irradiated a rotating <sup>176</sup>Yb target wheel to produce <sup>222</sup>U and <sup>221</sup>U in 4n and 5n de-excitation channels of the complete fusion reaction, respectively.

The evaporation residues (ER) were separated from the primary beam by TASCA and implanted into the stop detector consisting of two double-sided silicon-strip detectors. Two signals, one from each side of the stop detector were processed in two different parts of the ANDI system with a common trigger and zero suppression [1]. The signals from 144 vertical front strips were processed by analog amplifiers connected to peak-sensing ADCs [2]. The preamplified signals from 48 horizontal back strips were processed by sampling ADC's (FEBEX2) with 60 MHz frequency. Traces with total length of 50  $\mu$ s (7  $\mu$ s before and 43  $\mu$ s after) were recorded following an accepted trigger. The deadtime of the “analog” part was shorter than 43  $\mu$ s. Therefore it was always ready to accept the next triggered event [1]. Further, both data were combined into single events by an event builder of MBS [1].

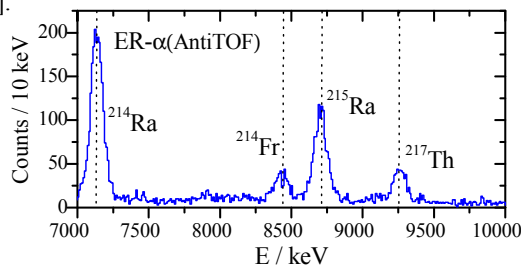


Fig 1: An energy spectrum of  $\alpha$ -particles from the ER- $\alpha$  correlation up to 14 s, with both events occurring in the same pixel.

An ER- $\alpha$  correlation analysis was performed to find recoiling nuclei and identify the measured  $\alpha$  lines (Fig. 1). Only  $\alpha$ -particle events were considered without a signal from the time-of-flight detector. Alpha decays of <sup>214</sup>Ra, <sup>215</sup>Ra, <sup>214</sup>Fr, and <sup>217</sup>Th were identified. From further analyses the decay of <sup>214</sup>Fr was found as a member of ER- $\alpha$ (7-18MeV)- $\alpha$ (<sup>214</sup>Fr) chains. The second member of this chain is typically a pile-up of two  $\alpha$  decays. These events were investigated using the data from the “digital” part. Clearly two signals were found in traces of them and  $\alpha$  decays of <sup>222</sup>Pa and <sup>218</sup>Ac were unambiguously determined (see Fig. 2a).

The traces of the ER's from ER- $\alpha$ (<sup>214</sup>Ra) were investigated in order to find “missing”  $\alpha$  decays of mother <sup>218</sup>Th and grandmother <sup>222</sup>U nuclei. In most cases only single signals were found, pointing to the implantation of <sup>214</sup>Ra. However, traces with two and three signals were also found (see Fig. 2b). These data allow us to unambiguously assign  $\alpha$  decays of <sup>218</sup>Th and <sup>222</sup>U.

The traces of the ER's from ER- $\alpha$ (<sup>217</sup>Th) were investigated to find the  $\alpha$  decay of the new nucleus <sup>221</sup>U. In most cases a single ER signal was seen. However, traces with two signals, which include the  $\alpha$  decay of the new nucleus <sup>221</sup>U, were also found (see Fig. 2c). More detailed information will be provided in [3].

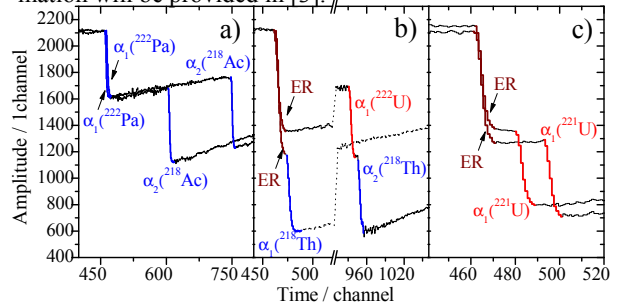


Fig 2: Example of traces of pile-up  $\alpha$ -particles correlated with <sup>214</sup>Fr a), ER's correlated with <sup>214</sup>Ra b), and with <sup>217</sup>Th c).

[1] N. Kurz et al., this Scientific Report (2012).

[2] J.M. Gates et al., Phys. Rev. C. 83 054618 (2011).

[3] J. Khuyagbaatar et al., to be published.

\* Work supported by HI Mainz

# Preparations towards X-Ray Fingerprinting of Element 115 Decay Chains\*

U. Forsberg<sup>1</sup>, P. Golubev<sup>1</sup>, L. G. Sarmiento<sup>2</sup>, J. Jeppsson<sup>1</sup>, D. Rudolph<sup>1</sup>, L.-L. Andersson<sup>3,4</sup>, D. Ackermann<sup>5</sup>, M. Asai<sup>6</sup>, M. Block<sup>5</sup>, K. Eberhardt<sup>7</sup>, J. Even<sup>4,7</sup>, Ch. E. Düllmann<sup>4,5,7</sup>, J. Dvorak<sup>4</sup>, J. M. Gates<sup>8</sup>, K. E. Gregorich<sup>8</sup>, R.-D. Herzberg<sup>3</sup>, F. P. Heßberger<sup>4,5</sup>, E. Jäger<sup>5</sup>, J. Khuyagbaatar<sup>4</sup>, I. Kojouharov<sup>5</sup>, J. V. Kratz<sup>7</sup>, J. Krier<sup>5</sup>, N. Kurz<sup>5</sup>, S. Lahiri<sup>9</sup>, B. Lommel<sup>5</sup>, M. Maiti<sup>9</sup>, E. Merchán<sup>5</sup>, J. P. Omtvedt<sup>10</sup>, E. Parr<sup>3</sup>, J. Runke<sup>5</sup>, H. Schaffner<sup>5</sup>, M. Schädel<sup>5,6</sup>, and A. Yakushev<sup>5</sup>

<sup>1</sup>Lund University, Lund, Sweden; <sup>2</sup>Universidad Nacional de Colombia, Bogotá, Colombia; <sup>3</sup>University of Liverpool, Liverpool, United Kingdom; <sup>4</sup>Helmholtz Institute Mainz, Mainz, Germany; <sup>5</sup>GSI Helmholtzzentrum für Schwerionenforschung, Darmstadt, Germany; <sup>6</sup>Advanced Science Research Center, Japan Atomic Energy Agency, Tokai, Japan; <sup>7</sup>Johannes Gutenberg-Universität Mainz, Mainz, Germany; <sup>8</sup>Lawrence Berkeley National Laboratory, Berkeley, USA; <sup>9</sup>Saha Institute of Nuclear Physics, Kolkata, India; <sup>10</sup>University of Oslo, Oslo, Norway

In preparation for an approved experiment aiming at X-ray fingerprinting of element 115 decay chains to unambiguously determine the atomic number of the involved nuclei, a number of final tests were performed in June 2011. The main experiment is designed to measure the energies of characteristic X-rays emitted following de-excitation via internal conversion in coincidence with  $\alpha$  decays into excited states.  $^{287}115$  will be produced in the  $^{243}\text{Am}(^{48}\text{Ca},4n)$  reaction, isolated in the gas-filled recoil separator TASCA [1], and guided to the TASI-Spec setup [2].

In this experiment we studied which of the two ion-optical modes of TASCA [1] is more beneficial to use together with TASI-Spec. Previously, TASI-Spec has been used with TASCA in the “Small image mode” (SIM) with good results. However, simulations and experiments [4] have shown that insertion of slits inside TASCA can decrease the background in “High transmission mode” (HTM) significantly. To investigate the performance of TASI-Spec with TASCA in HTM, the reaction  $^{208}\text{Pb}(^{48}\text{Ca},2n)^{254}\text{No}$  was used (for details, see [3]). First, the previously determined optimal TASCA SIM quadrupole magnet settings for TASI-Spec were confirmed to yield the maximum transmission. Secondly, a series of HTM tests using the nominal TASCA focal-plane detector confirmed that a strong background suppression can be achieved by inserting slits in TASCA. Thirdly, the HTM magnet settings were optimized to give the best transmission of  $^{254}\text{No}$  into TASI-Spec. This optimization was guided by simulations [5] of the trajectories of  $^{254}\text{No}$  through TASCA. Relative experimental transmissions were derived from the number of events recorded in the  $\alpha$  peak from  $^{254}\text{No}$  in the TASI-Spec implantation detector, normalized to the beam integral. The optimal settings were found within the range of magnet settings suggested by the simulations.

The spacial distribution of  $^{254}\text{No}$  events over the TASI-Spec implantation detector with TASCA in HTM is illustrated in Fig. 1(b), showing data from a simulation of the

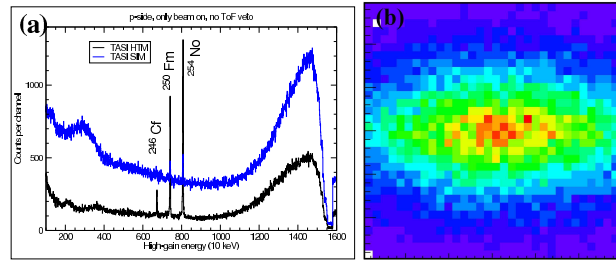


Figure 1: (a) Energy spectra accumulated using SIM (blue) and HTM (black). (b) Simulated distribution, in HTM, of  $^{254}\text{No}$  in the TASI-Spec implantation detector [3].

experiment. The implantation profile is elongated in the horizontal direction, as expected in HTM. Since the ions have to pass a cylindrical tube on their way to TASI-Spec, the best use of the two focusing quadrupoles turned out to be when the horizontal focusing is somewhat stronger than the vertical one. The optimized settings established in this experiment can be used for determining how to tune the magnets in other experiments using TASI-Spec with HTM.

The transmission to TASI-Spec with TASCA in HTM was  $\sim 80\%$  of the one achieved in SIM. The main advantage in HTM is the excellent background suppression. Fig. 1(a) shows beam-on energy spectra from SIM (blue) and HTM with slits inserted (black). The clean HTM spectrum implies that it is possible to search for  $\alpha$ -X-ray coincidences in the beam-on periods as well as in the beam-off periods, even without using a veto detector, such as a MWPC, for implanted particles. In SIM, only beam-off data can be used when no MWPC is installed, due to too high background rates during beam-on periods. Since the beam-on data accounts for 25% of the events due to the duty cycle of the beam, the total amount of TASI-Spec data is comparable for HTM and SIM.

## References

- [1] A. Semchenkov *et al.*, Nucl. Instr. Meth. **B266**, 4153 (2008)
- [2] L.-L. Andersson *et al.*, Nucl. Instr. Meth. **A622**, 164 (2010)
- [3] U. Forsberg *et al.*, Acta Phys. Pol. B, in press
- [4] J. M. Gates *et al.*, contribution to this report
- [5] K. E. Gregorich *et al.*, GSI Scientific Report, 144 (2006)

\*This work was co-funded by the European Commission under the capacities program (Grant Agreement Number FP7-227867, ENSAR), and supported by the Helmholtz Institute Mainz. We also thank the Royal Physiographical Society in Lund for funding of equipment.

# IRiS - Feasibility Calculations

J. Dvorak<sup>1</sup> and Ch.E. Düllmann<sup>1,2,3</sup>

<sup>1</sup>Helmholtz Institut Mainz, Mainz, Germany; <sup>2</sup>Univ. Mainz, Mainz, Germany; <sup>3</sup>GSI Darmstadt, Germany.

The design for a new Inelastic Reactions Isotope Separator (IRiS) [1] to be installed at the GSI Darmstadt has been developed in a joint effort of an international collaboration, headed by the University Mainz, the Helmholtz Institute Mainz, and the GSI. This separator will be dedicated to the investigation of neutron-rich isotopes of heavy and superheavy elements, which can be produced exclusively in multi-nucleon transfer reactions. So far, experimental studies of transfer products with recoil separators have focused on light isotopes not far from stability for a number of reasons. These include low efficiencies for multi-nucleon transfer reactions of recoil separators that are optimized for fusion-evaporation reactions. Here, we present developments toward a dedicated facility featuring an extra-large angular acceptance separator IRiS, which will make the study of heavy neutron-rich transfer reaction products feasible.

The task of IRiS is to separate reaction products of interest from the primary beam and unwanted byproducts. The separated products will be delivered either into a detector setup or alternatively to auxiliary setups for identification and further investigation of the species of interest. For internal detection in a Si stop detector, maximum acceptable count rates are on the order of 1 kHz. For detection in auxiliary systems like a gas stopping chamber for coupling to external experimental setups, count rates up to 100 kHz appear acceptable.

In our feasibility calculations, two particular nuclear reactions were studied in detail: the reaction  $^{48}\text{Ca} + ^{248}\text{Cm}$  at a center-of-mass beam energy  $E_{\text{CM}} = 209$  MeV, and the reaction  $^{238}\text{U} + ^{248}\text{Cm}$  at  $E_{\text{CM}} = 750$  MeV. Predictions for the multi-nucleon transfer channels from theoretical models of V. Zagrebaev [2] and G. Adamian and N. Antonenko [3] were used for these studies. An ion-optical simulation was developed in framework of this study to test the performance of various potential IRiS setups for the two selected reactions. Besides the heavy n-rich products of interest, other reaction byproducts were simulated as well as they will be the major source of background.

Due to large differences in the properties (e.g., velocity, energy, angular emittance) of the studied heavy transfer products when produced in different reactions, the optimal setup differs for either of the reactions. The most versatile setup was found to be one based on a superconducting solenoid magnet as the main component, with a stored energy of  $E \sim 10$  MJ. In the simulations, a solenoid magnet with a maximum magnetic field strength of  $B_{\text{max}}=4.3$  T and dimensions of 2 m length and 90 cm inner diameter was used. The target is located on axis at the entrance of the solenoid. A beam dump blocking central ions is placed axially at the exit of the solenoid and the detector is located further downstream from the solenoid,

see Fig. 1. Ion-optical simulations of the identified optimal setups resulted in efficiencies of roughly 20% for separation of the heaviest ( $Z \geq 102$ ) transfer products, while keeping the background rate well below 100 kHz. For the reaction  $^{238}\text{U} + ^{248}\text{Cm}$ , the background is predicted to be below 1 kHz, when using a  $500\text{-}\mu\text{g}/\text{cm}^2$  thick target. Using thicker targets resulted in increased background. For the reaction  $^{48}\text{Ca} + ^{248}\text{Cm}$  two setups were investigated. The setup tuned for detection of the heaviest ( $Z \geq 102$ ) transfer products resulted in background below 1 kHz and the possibility to roughly identify  $A$  and  $Z$  of the ions. When the setup was adjusted for the detection of  $\text{Fm}$  isotopes, the background increased to  $\sim 10$  kHz.

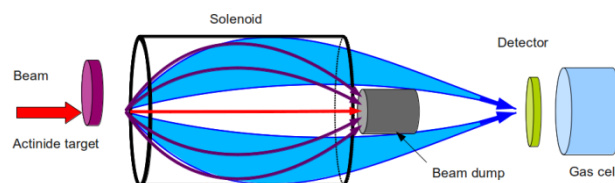


Figure 1: Schematic drawing of a solenoid-based IRiS design in an asymmetric mode. A thin actinide target is bombarded with a heavy-ion beam. A beam dump located on axis behind the solenoid stops both, beam ions, which pass through the target without undergoing nuclear reactions (red arrow) as well as light products of transfer reaction channels (violet). Heavy transfer reaction products (blue) are focused on a disk-like detector at the exit of the solenoid. In the separator mode, the detector is removed, and the products pass through a thin window into the gas-filled stopping cell, where they are available for transport to ancillary setups.

We conclude that the optimal identified setups perform better than expected for the reactions of choice. These setups will most probably not only allow for delivery of separated products into a gas stopping cell, which is the main design requirement, but also enable on-line detection in internal Si detectors. The above described setups offer enough space for inserting of multiple gas-filled detectors for precise TOF measurement and ideally also for a rough  $Z$  identification.

## References

- [1] J. Dvorak et al., Nucl. Instrum. Meth. A 652 (2011) 687.
- [2]
- [3]

# Mass Measurements of heavy actinides with SHIPTRAP\*

*E. Minaya Ramirez*<sup>1,2</sup>, *D. Ackermann*<sup>2</sup>, *K. Blaum*<sup>3,4</sup>, *M. Block*<sup>2</sup>, *C. Droese*<sup>5</sup>, *Ch. E. Düllmann*<sup>1,2,6</sup>, *M. Dworschak*<sup>2</sup>, *M. Eibach*<sup>6</sup>, *S. Eliseev*<sup>3</sup>, *E. Haettner*<sup>2,7</sup>, *F. Herfurth*<sup>2</sup>, *F.P. Heßberger*<sup>1,2</sup>, *S. Hofmann*<sup>2</sup>, *J. Ketelaer*<sup>3</sup>, *J. Ketter*<sup>3</sup>, *G. Marx*<sup>5</sup>, *D. Nesterenko*<sup>8</sup>, *Yu. Novikov*<sup>8</sup>, *W.R. Plass*<sup>2,7</sup>, *D. Rodríguez*<sup>10</sup>, *C. Scheidenberger*<sup>2,7</sup>, *L. Schweikhard*<sup>5</sup>, *P.G. Thirolf*<sup>11,\*</sup>, *G.K. Vorobjev*<sup>2,8</sup>, and *C. Weber*<sup>11,\*</sup>

<sup>1</sup>Helmholtz-Institut Mainz; <sup>2</sup>GSI Helmholtzzentrum für Schwerionenforschung, Darmstadt; <sup>3</sup>Max-Planck-Institut für Kernphysik, Heidelberg; <sup>4</sup>Ruprecht-Karls-Universität Heidelberg; <sup>5</sup>Ernst-Moritz-Arndt-Universität, Greifswald; <sup>6</sup>Johannes Gutenberg-Universität Mainz; <sup>7</sup>Justus-Liebig-Universität Gießen; <sup>8</sup>PNPI RAS Gatchina, St. Petersburg; <sup>10</sup>Universidad de Granada; <sup>11</sup>Ludwig-Maximilians-Universität München

Masses in the region of the heaviest elements could previously only be derived indirectly by linking mass differences between nuclides and their decay products using measured  $\alpha$ -decay energies. However this approach depends on the knowledge of nuclear level schemes. In contrast, direct mass measurements yield absolute mass values, binding energies and provide anchor points to pin down  $\alpha$ -decay chains. This is especially important for odd-odd and odd-A nuclides, where the  $\alpha$  decay typically populates excited states. In the absence of complete and quantitative information of the nuclear structure, no unambiguous mass determination is possible. Mass measurements of nuclides, e.g., around <sup>254</sup>No allow determining the masses of nuclides located in the superheavy element region.

Nuclides above fermium can only be produced at very low rates. Nonetheless, recently the first direct measurements on transuranium nuclides have been performed with SHIPTRAP [1]. The obtained accurate mass values provided anchor points to fix  $\alpha$ -decay chains passing through the nobelium isotopes <sup>252–254</sup>No [2]. The measurements have now been extended to further even more exotic nuclides, namely <sup>255</sup>No and <sup>255–256</sup>Lr. The radionuclides were produced and separated from the primary beam by the velocity filter SHIP. Fusion-evaporation reactions of a <sup>48</sup>Ca beam with lead and bismuth targets were used to produce different nobelium and lawrencium isotopes with cross sections as low as about 50 nb. Evaporation residues were guided to SHIPTRAP. In a first step their energy was decreased from tens of MeV to a few eV using a buffer-gas filled stopping cell. Afterwards they were injected into a 7-Tesla double-Penning-trap system. The mass was determined by measuring the cyclotron frequency  $\nu_c = qB/(2\pi m)$  of the ions using a time-of-flight ion-cyclotron-resonance detection technique. An important development to substantially reduce long-term fluctuations of the magnetic field [3] allowed the recording of a single resonance over a period of 4 days in the case of <sup>256</sup>Lr. This measurement represents a significant breakthrough towards direct mass measurements of superheavy nuclides.

\* Work supported by the BMBF (06ML236I, 06ML9148, 06GF9103I, RUS-07/015), Rosminnauki (2.2.1), GSI (Grant GFMARX1012), the Max-Planck Society, and the Research Center Elementary Forces, Mathematical Foundations and the Helmholtz Institute Mainz

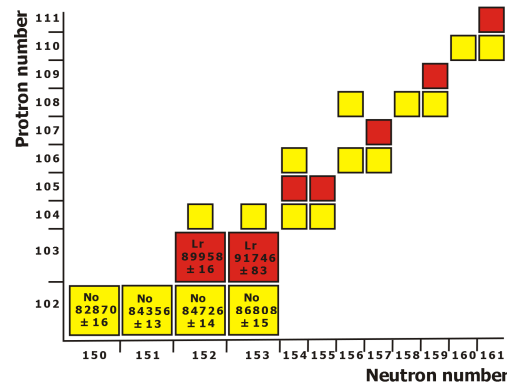


Figure 1: Decay chains linked to the direct mass measurements from this work. The mass excess is indicated in keV.

In the Atomic-Mass Evaluation 2003, the masses of the lawrencium isotopes <sup>255,256</sup>Lr were only estimated from systematic trends. The combination of our direct mass measurements with spectroscopic data allows determining the masses of superheavy nuclides (see Fig 1). The masses of  $\alpha$ -decay chains starting with even-even nuclides, as for example <sup>270</sup>Ds ( $Z = 110$ ), are now established with low uncertainties. For the first time we also provide anchor points for nuclides with an odd number of protons. Moreover, the new mass value from <sup>255</sup>No complement our previous results on the neutron-rich side of the  $N = 152$  deformed shell. Thus our experimental binding energies provide precise values for the two-neutron separation energies  $S_{2n}$ . This allows mapping the deformed shell gap at  $N = 152$ , which is connected to the predicted spherical shell gap at  $N = 184$  as it originates from the the same single-particle orbitals. Therefore the results obtained with SHIPTRAP enhance our knowledge of shell effects nearby the predicted island of stability.

## References

- [1] M. Block et al., Nature 463 (2010) 785.
- [2] M. Dworschak et al., Phys. Rev. C 81 (2010) 064312.
- [3] C. Droese et al., Nucl. Instrum. Meth. A 632 (2011) 157.

# Metal carbonyl complexes – a new compound class accessible for transactinides\*

J. Even<sup>1,2</sup>, A. Yakushev<sup>3</sup>, Ch.E. Düllmann<sup>1,2,3</sup>, J. Dvorak<sup>2</sup>, R. Eichler<sup>4</sup>, O. Gothe<sup>5</sup>, D.Hild<sup>1</sup>, E. Jäger<sup>3</sup>, J. Khuyagbaatar<sup>2,3</sup>, J.V. Kratz<sup>1</sup>, J. Krier<sup>3</sup>, L. Niewisch<sup>1</sup>, H. Nitsche<sup>5</sup>, I. Pysmenetska<sup>1</sup>, M. Schädel<sup>3,7</sup>, B. Schausten<sup>3</sup>, A. Türler<sup>4,6</sup>, N. Wiehl<sup>1</sup>, D. Wittwer<sup>4,6</sup>

<sup>1</sup>University Mainz, Mainz, Germany; <sup>2</sup>HIM, Mainz, Germany; <sup>3</sup>GSI, Darmstadt, Germany; <sup>4</sup>PSI, Villigen, Switzerland, <sup>5</sup>LBNL, Berkeley, CA, USA; <sup>6</sup>University of Berne, Berne, Switzerland; <sup>7</sup>JAEA, Tokai, Japan

Gas-phase chemical studies of transactinide elements were so far restricted to simple, thermally stable, inorganic compounds. Metal-carbonyl complexes would provide a link to metal-organic chemistry. Binary, mononuclear, volatile carbonyl complexes are known for all lighter elements of group 6 and 8 of the periodic table. Seaborgium hexacarbonyl has been predicted to be stable [1]. Its experimental study would be interesting, because relativistic effects are predicted to influence the metal-CO bond.

We explored the method of rapid in-situ synthesis of transition-metal carbonyl complexes with short-lived isotopes. First tests were performed at the TRIGA Mainz reactor, using the <sup>249</sup>Cf(n,f) reaction. Recoiling fission products were thermalized either in pure N<sub>2</sub> or in a CO/N<sub>2</sub>-mixture. All volatile compounds were transported in a gas stream to an activated charcoal trap, which was monitored with a  $\gamma$ -ray detector. Figure 1 shows a typical spectrum from the CO/N<sub>2</sub> measurements.

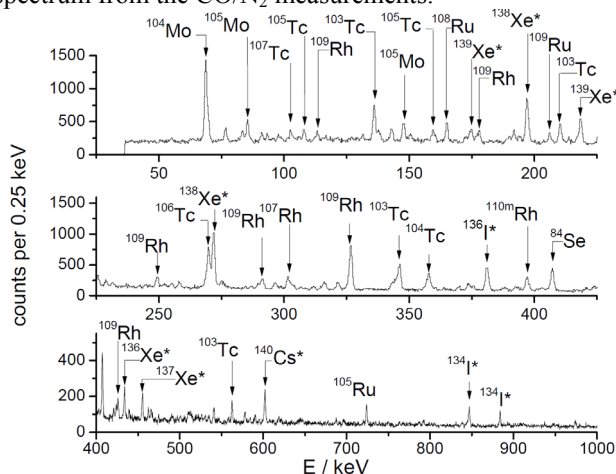


Figure 1:  $\gamma$ -ray spectrum of fission products transported in a CO/N<sub>2</sub> mixture collected for 2 min in a charcoal trap. Subsequently, the sample was measured for 2 min.  $\gamma$ -lines, which were also visible in spectra of pure N<sub>2</sub> experiments, are marked with \*.

Short-lived isotopes of Se, Mo, Tc, Ru and Rh were only observed in the spectra when CO was added. These elements form volatile compound with the CO. Transport with cluster (aerosol) material can be excluded.

To test this method under experimental conditions relevant for transactinides,  $\alpha$ -decaying <sup>163</sup>W, <sup>164</sup>W, <sup>170</sup>Os and <sup>171</sup>Os were produced in <sup>144</sup>Sm(<sup>24</sup>Mg,4-5n) and <sup>152</sup>Gd(<sup>24</sup>Mg,4-5n) reactions at the gas-filled recoil separa-

\* Work supported by the Helmholtz Institute Mainz, the Research Center Elementary Forces and Mathematical Foundations (EMG), the BMBF under contract No. 06MZ223I, and the Swiss National Science Foundation under contract No. 200020 126639 #evenj@uni-mainz.de

tor TASCA. Evaporation residues were separated from the primary beam and from unwanted transfer products within TASCA. They were thermalized in mixtures of He and CO in a Recoil Transfer Chamber (RTC) [2] at the TASCA focal plane. Volatile carbonyl complexes – most likely Os(CO)<sub>5</sub> and W(CO)<sub>6</sub> – were formed in the RTC and were transported with the gas stream to the thermochromatography detector COMPACT [3]. The COMPACT detector array is a chromatography channel consisting of SiO<sub>2</sub> covered PIN diodes, suitable to register  $\alpha$  particles emitted from volatile species inside the channel. A negative temperature gradient was applied along the chromatography column. Figure 2 shows thermochromatograms of Os(CO)<sub>5</sub> and W(CO)<sub>6</sub>. The measurements are compared to Monte Carlo Simulations. From the deposition patterns of W and Os, adsorption enthalpies of W(CO)<sub>6</sub> of  $(-46.5 \pm 2.5)$  kJ/mol and  $(-43^{+3.5}_{-2.5})$  kJ/mol for Os(CO)<sub>5</sub> were deduced. These values indicate physisorption of these carbonyl complexes on SiO<sub>2</sub>.

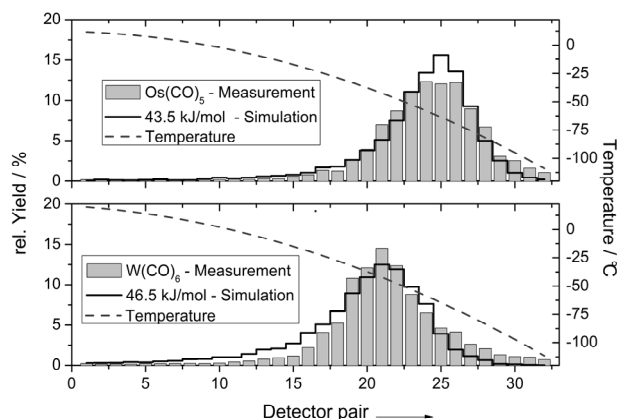


Figure 2: Upper graph: combined thermochromatogram of <sup>170</sup>Os(CO)<sub>5</sub> and <sup>171</sup>Os(CO)<sub>5</sub>. Lower graph: combined thermochromatogram of <sup>163</sup>W(CO)<sub>6</sub> and <sup>164</sup>W(CO)<sub>6</sub>.

Based on the results of our experiments, Sg(CO)<sub>6</sub> and Hs(CO)<sub>5</sub> are now within reach for transactinide chemistry. These compounds are suitable for chemical characterization by thermochromatography and appear highly promising for nuclear spectroscopy under low background conditions.

## References

- [1] C. S. Nash, B. E. Bursten, J. Am. Chem. Soc. **121** (1999) 10830.
- [2] J. Even et al., Nucl. Instr. Meth. A. **638**, (2011) 157.
- [3] J. Dvorak et al., Phys. Rev. Lett. **100** (2008) 132503.

# Development of an on-line high-temperature surface ion source for fission products at TRIGA-SPEC\*

D. Renisch<sup>1</sup>, T. Beyer<sup>2,3</sup>, K. Blaum<sup>2,3</sup>, Ch. E. Düllmann<sup>1,4,5</sup>, K. Eberhardt<sup>1</sup>, M. Eibach<sup>1,2</sup>, S. Klein<sup>1</sup>, Sz. Nagy<sup>2,4</sup>, W. Nörtershäuser<sup>1,4,5</sup>, C. Smorra<sup>1,2,3</sup>, and the TRIGA-SPEC collaboration

<sup>1</sup>Institut für Kernchemie, Johannes Gutenberg-Universität, Mainz, Germany; <sup>2</sup>Max-Planck-Institut für Kernphysik, Heidelberg, Germany; <sup>3</sup>Ruprecht Karls-Universität, Heidelberg, Germany; <sup>4</sup>GSI Helmholtzzentrum für Schwerionenforschung, Darmstadt, Germany; <sup>5</sup>Helmholtz-Institut Mainz, Germany

Precise knowledge of nuclear properties like binding energies, nuclear spins and moments or charge radii is essential to obtain a detailed understanding of nuclear structure. The TRIGA-SPEC facility [1] allows to determine these properties by investigating stable nuclides, long-lived actinide isotopes and neutron-rich fission products. An on-line ion source, based on the ion source of the HELIOS mass separator setup [2], was recently installed and tested.

Short-lived neutron-rich isotopes are produced in the neutron-induced fission of, e.g., <sup>235</sup>U at the TRIGA Mainz research reactor. The fission products are thermalized in a gas-filled recoil chamber, which is flushed with the gas seeded with KCl aerosol particles, on which non-volatile fission products adsorb. They are rapidly transported with the gas flow through a capillary (1 mm ID) to the on-line ion source [3].

The first part of the source is a cone-shaped skimmer to remove the carrier gas while the aerosol particles enter the source. The main part of the source consists of a tungsten tube, which is heated up by electron bombardment to temperatures above 2000°C. Aerosol particles inside the source break up and fission products are released and ionized by surface ionization. This method works well for alkaline, alkaline earth and rare earth elements. The ions are subsequently extracted and accelerated by high voltage (30 kV) towards a 90°-dipole-magnet which is used for mass separation. Behind the magnet, several detection systems (Faraday Cup (FC), Si-Detector, Microchannel plate (MCP)) are available for beam monitoring.

In a first run, two mass spectra were recorded with the FC (Figure 1), with and without gasjet. Ions of alkaline elements (Na<sup>+</sup>, K<sup>+</sup>, Rb<sup>+</sup>) were detected as expected. The K<sup>+</sup> signal increases significantly when the gasjet is turned on because of the large number of KCl particles entering the source.

In a second step a Si-Detector was used to detect the  $\beta$ -decay of fission products. The focus was on Rb isotopes, because they are produced with high yield and can be easily ionized. The signal of the Si-Detector had only a weak background signal (about 1ct/s). While scanning through the mass region of Rb, significant increases in the count rate were observed. Around mass 92 and 93 count rates of up to 5-20 cts/s were achieved. This corresponds to the short-lived isotopes <sup>92</sup>Rb and <sup>93</sup>Rb with half-lives of 4.5 s and 5.8 s. <sup>92</sup>Rb was collected for about 45 min by implantation into an Al foil. Afterwards, the decay

products (Sr and Y isotopes) were detected by a  $\gamma$ -measurement (Figure 2). This measurement demonstrates for the first time the ionization of fission products at the TRIGA-SPEC facility. Future work will focus on improving the overall efficiency and stability of the setup.

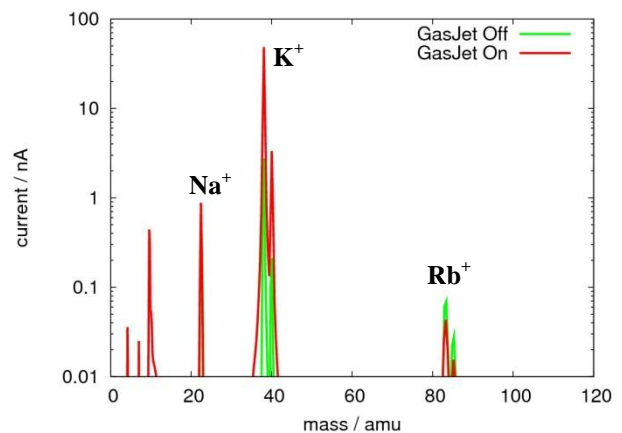


Figure 1. Mass spectrum behind the dipole magnet recorded with a Faraday Cup.

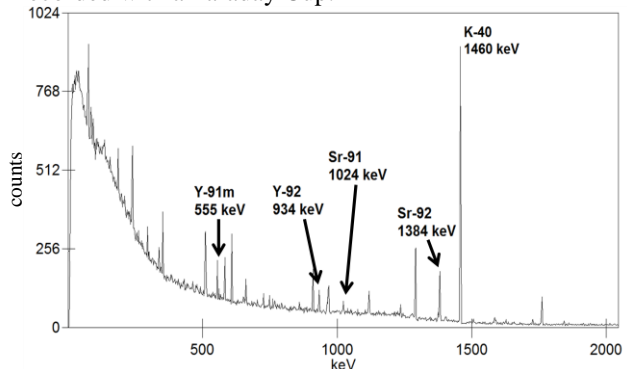


Figure 2.  $\gamma$ -spectrum of collected <sup>91</sup>Rb and <sup>92</sup>Rb isotopes. Due to the short half-life of the Rb isotopes, the decay products Sr and Y were detected.

## References

- [1] J. Ketelaer, et al., Nucl. Inst. Meth. A 594 (2008) 162
- [2] A. Mazumdar, et al., Nucl. Inst. Meth. 174 (1980) 183
- [3] A. Mazumdar, et al., Nucl. Inst. Meth. 186 (1981) 131

\* Financial support by the Max-Planck Society, by BMBF (06MZ91721), the Research Center "Elementary Forces and Mathematical Foundations" (EMG), and Stiftung Rheinland-Pfalz für Innovation (961-386261/854) is acknowledged.

# Resonance conditions of neutrinoless double-electron capture in cadmium and osmium isotopes investigated at TRIGA-TRAP

C. Smorra<sup>1,2,3</sup>, T. Beyer<sup>1,2</sup>, K. Blaum<sup>1,2</sup>, M. Block<sup>4</sup>, Ch. E. Düllmann<sup>3,4,5</sup>, K. Eberhardt<sup>3</sup>, M. Eibach<sup>2,3</sup>, S. Eliseev<sup>1</sup>, Sz. Nagy<sup>1,4</sup>, W. Nörtershäuser<sup>3,4</sup> and D. Renisch<sup>1,3</sup>

<sup>1</sup>Max-Planck-Institut für Kernphysik, D-69117 Heidelberg; <sup>2</sup>Fakultät für Physik und Astronomie, Ruprecht-Karls-Universität, D-69120 Heidelberg; <sup>3</sup>Institut für Kernchemie, Johannes Gutenberg-Universität, D-55099 Mainz; <sup>4</sup>GSI Helmholtzzentrum für Schwerionenforschung, D-64291 Darmstadt; <sup>5</sup>Helmholtz-Institut Mainz, D-55099 Mainz.

**Introduction and motivation:** An open question in neutrino physics is whether the neutrino is its own antiparticle, i.e. of Majorana type. The observation of a neutrinoless double-beta transition could give the answer to that question [1]. However, such transitions are difficult to observe due to their long half-life. For nuclides undergoing double-electron capture, the decay rate is resonantly enhanced in case of an energy degeneracy of the ground state of the mother nuclide and the nuclear and/or atomic excited state of the daughter nuclide [2, 3]. In this case the double-electron capture can take place without the emission of an additional photon to carry away the excess energy, which leads to a significantly higher decay rate. The resonance condition for double-electron capture is fulfilled if the excess energy  $\Delta = (Q - E_\gamma - B_{2h})$  is smaller than the sum of widths of the two-electron-hole state and the nuclear excited state of the daughter nucleus  $\Gamma_{2h}$ .  $Q$  denotes the  $Q$ -value, i.e. the mass difference of the atomic masses ( $M_m - M_d$ ) of the mother and daughter nuclides,  $E_\gamma$  the nuclear excitation energy, and  $B_{2h}$  is the energy of the double-electron hole state. The uncertainty of the  $Q$ -value is often the limitation for the identification of resonantly enhanced transitions. High-precision measurements of the  $Q$ -value with Penning-trap mass spectrometers such as TRIGA-TRAP [4] can provide direct measurements of double-electron capture  $Q$ -values with the precision of a few hundred electron volts or better [5]. Thereby, resonantly enhanced transitions can be identified. In 2011 we have investigated three double-electron capture  $Q$ -values of the transitions  $^{106}\text{Cd}$ - $^{106}\text{Pd}$ ,  $^{108}\text{Cd}$ - $^{108}\text{Pd}$ , and  $^{184}\text{Os}$ - $^{184}\text{W}$ .

**Experimental setup and results:** The mass and  $Q$ -value measurements were performed offline with TRIGA-TRAP using the laser ablation ion source [6] equipped with cadmium, palladium and tungsten foils with natural isotopic abundance. Due to the low isotopic abundance of  $^{184}\text{Os}$  (0.02%) a target was prepared from a sample enriched in  $^{184}\text{Os}$  (1.5% abundance) and pressed into a pellet using silver powder as adhesive material. The  $Q$ -values were measured by recording alternately the cyclotron frequency of the mother and daughter nuclide with the time-of-flight ion-cyclotron resonance (TOF-ICR) method. A Ramsey excitation scheme was used with two excitation pulses of 100 ms and a waiting time of 800 ms in between for cadmium and palladium, and two excitation pulses of 200 ms excitation and 1600 ms waiting time for osmium and tungsten. The  $Q$ -value is obtained from the frequency ratio  $r = \nu_m/\nu_d$  from the mother to the daughter nuclide:

$$Q = M_m - M_d = (M_m - m_e)(1 - r),$$

where  $m_e$  denotes the electron mass. The  $Q$ -values obtained from the measurements are listed in Table 1.

Transition	$Q_{exp} / \text{keV}$	$Q_{AME2003} / \text{keV}$
$^{106}\text{Cd}$ - $^{106}\text{Pd}$	2775.01 (0.56)	2770 (6)
$^{108}\text{Cd}$ - $^{108}\text{Cd}$	272.04 (0.55)	272 (7)
$^{184}\text{Os}$ - $^{184}\text{W}$	1453.68 (0.58)	1451.2 (1.0)

Table 1:  $Q$ -values of double-electron capture transitions determined by TRIGA-TRAP and the literature  $Q$ -value from the Atomic-Mass Evaluation (AME) 2003.

$Q$ -values of three double-electron capture transitions were determined. In case of  $^{106}\text{Cd}$  the  $Q$ -value from a previous experiment [7] was confirmed. An energy degeneracy to an excited (2, 3)<sup>-</sup> state at 2748.2(4) keV excitation energy was found [7, 8], but the decay rate is suppressed due to the negative parity of the excited state and the double-electron capture probability from  $\text{KL}_3$  orbitals. The  $Q$ -values of the double-electron capture in  $^{108}\text{Cd}$  and  $^{184}\text{Os}$  were measured by Penning-trap mass spectrometry for the first time and their uncertainties were reduced. No resonant enhancement was found for  $^{108}\text{Cd}$ .  $^{184}\text{Os}$  has an excited 0<sup>+</sup> state at 1322.152(22) keV excitation energy and an energy excess of 11.3(1.0) keV for the capture of two K-shell electrons. The upper limit for the half-life predicted for this transition is about 10<sup>27</sup> years [8], which is rather short compared to other double-electron capture transitions. Our measurement yields a smaller excess energy of 8.83 (0.58) keV suggesting the half-life to be shorter. Our data will be useful for a recalculation of the half-life.

**Conclusion and outlook:** Three  $Q$ -values of double-electron capture nuclides were measured. For  $^{106}\text{Cd}$  the value from [7] was confirmed. For  $^{108}\text{Cd}$  and  $^{184}\text{Os}$ , the uncertainty was significantly improved. Our result can be used to recalculate the half-life of  $^{184}\text{Os}$  in order to decide whether it is a suitable nuclide to observe the neutrinoless double-electron capture.

## References

- [1] Avignone F. T. *et al.*, Rev. Mod. Phys. 80, 481, 2008.
- [2] Voloshin M. B. *et al.*, JETP Lett. 35, 656, 1982.
- [3] Bernabeu J. *et al.*, Nucl. Phys. B 223, 15, 1983.
- [4] Ketelaer J. *et al.*, Nucl. Instr. Meth. A 594 162-177, 2008.
- [5] Blaum K., Phys. Rep. 425 1-78, 2006.
- [6] Smorra C. *et al.*, J. Phys. B 42, 154028, 2009.
- [7] Goncharov M. *et al.*, Phys. Rev. C 84, 028501, 2011.
- [8] Krivoruchenko M.I. *et al.*, Nucl. Phys. A 859, 140-171, 2011.
- [9] Audi G. *et al.*, Nucl. Phys. A 729, 337-676, 2003.

## Acknowledgements

Financial support is acknowledged from the Max-Planck Society as well as support of the technical staff of the TRIGA Mainz reactor at the University of Mainz. Sz. Nagy acknowledges the support of the Alliance Program of the Helmholtz Association (HA216/EMMI). We also thank D. Beck and F. Herfurth from GSI/Darmstadt, and the CS developer team for their support.